Impact of Winds and Southern Ocean SSTs on Antarctic Sea Ice Trends and Variability®

EDWARD BLANCHARD-WRIGGLESWORTH, A LETTIE A. ROACH, AARON DONOHOE, AND QINGHUA DINGC

^a Department of Atmospheric Sciences, University of Washington, Seattle, Washington

^b Polar Science Center, Applied Physics Laboratory, University of Washington, Seattle, Washington

^c Department of Geography, Earth Research Institute, University of California Santa Barbara, Santa Barbara, California

(Manuscript received 27 May 2020, in final form 23 October 2020)

ABSTRACT: Antarctic sea ice extent (SIE) has slightly increased over the satellite observational period (1979 to the present) despite global warming. Several mechanisms have been invoked to explain this trend, such as changes in winds, precipitation, or ocean stratification, yet there is no widespread consensus. Additionally, fully coupled Earth system models run under historic and anthropogenic forcing generally fail to simulate positive SIE trends over this time period. In this work, we quantify the role of winds and Southern Ocean SSTs on sea ice trends and variability with an Earth system model run under historic and anthropogenic forcing that nudges winds over the polar regions and Southern Ocean SSTs north of the sea ice to observations from 1979 to 2018. Simulations with nudged winds alone capture the observed interannual variability in SIE and the observed long-term trends from the early 1990s onward, yet for the longer 1979–2018 period they simulate a negative SIE trend, in part due to faster-than-observed warming at the global and hemispheric scale in the model. Simulations with both nudged winds and SSTs show no significant SIE trends over 1979–2018, in agreement with observations. At the regional scale, simulated sea ice shows higher skill compared to the pan-Antarctic scale both in capturing trends and interannual variability in all nudged simulations. We additionally find negligible impact of the initial conditions in 1979 on long-term trends.

KEYWORDS: Antarctica; Sea ice; Atmosphere-ocean interaction; Climate models

1. Introduction

Antarctic sea ice is characterized by large interannual variability and a small long-term increase in areal coverage since 1979 (e.g., Comiso et al. 2017; Eisenman et al. 2014) despite an abrupt reduction in sea ice cover since 2016 (Parkinson 2019). The observed record represents the combined effects of natural modes of atmosphere, ocean, and cryosphere internal variability, the response to stratospheric ozone depletion, and the response to global warming, and much work has focused on the mechanisms driving the overall small positive trend in Antarctic sea ice cover that has occurred despite an increase in global mean surface temperature. Some of the proposed mechanisms are (i) intensified Southern Ocean westerlies due to ozone depletion (Thompson and Solomon 2002) leading to sea ice expansion (Turner et al. 2009) via equatorward Ekman ice transport, although the same enhanced surface westerlies cause sea ice retreat at longer time scales (Sigmond and Fyfe 2010; Bitz and Polvani 2012) due to increased upwelling of warmer subsurface waters by Ekman suction (Ferreira et al. 2015); (ii) reduced interaction between the surface ocean and the subsurface warm waters due to increased ocean stratification as a result of freshwater discharge from Antarctic land ice (Bintanja et al. 2013;

Supplemental information related to this paper is available at the Journals Online website: https://doi.org/10.1175/JCLI-D-20-0386.s1.

Corresponding author: Edward Blanchard-Wrigglesworth, ed@ atmos.washington.edu

Bronselaer et al. 2018), decreased surface salt input via brine rejection (Zhang 2007), or increased regional precipitation (Liu and Curry 2010); (iii) delayed warming of the Southern Ocean relative to the rest of the globe due to the basic-state ocean overturning circulation (Armour et al. 2016); (iv) changes in winds that increase ice production in regions of anomalous wind convergence (Zhang 2014) and northward ice advection (Holland and Kwok 2012); (v) random occurrences of natural variability (Polvani and Smith 2013); (vi) tropically driven atmospheric circulation trends over West Antarctica that are responsible for the recent expansion (e.g., Meehl et al. 2016; Purich et al. 2016); (vii) changes in ocean waves impinging on the sea ice, with smaller swells promoting sea ice expansion and vice versa (Kohout et al. 2014); and (viii) internal variability of Southern Ocean convection (Zhang et al. 2019). The cause of the drastic reduction in sea ice in 2016 has been ascribed to anomalous winds in the spring of 2016 (Stuecker et al. 2017; Schlosser et al. 2018) that in part resulted from tropically driven teleconnections (Purich and England 2019), and this reduction in sea ice has persisted since 2016 due to a warmer upper Southern Ocean (Meehl et al. 2019).

There is no consensus on a mechanistic understanding of the processes that drive Antarctic sea ice variability and trends. Climate models in phase 5 of the Coupled Model Intercomparison Project (CMIP5) both tend to show large biases in their Antarctic sea ice mean state and have been unable to reproduce observed long-term sea ice increases since 1979, instead simulating ice loss over this time period (e.g., Turner et al. 2013). This model—observational mismatch persists in the new CMIP6 suite of models (Roach et al. 2020). It is unclear why models are unable to simulate observed trends

(e.g., Hobbs et al. 2016), and biases in the trends of atmospheric circulation and its coupling to sea ice may partly be responsible (e.g., Holland et al. 2017b). Indeed, trends in winds in CMIP5 are generally weaker than those in observations (Mahlstein et al. 2013), and the coupling between the southern annular mode (SAM) and sea ice appears to be weaker in the models (Schroeter et al. 2017) but also shows large model uncertainty (Holland et al. 2017a). Additionally, pervasive upper ocean warming in models may also limit their ability to simulate positive sea ice extent (SIE) trends (Schneider and Deser 2018), while sea ice trends are coupled to warming global temperature trends, which themselves tend to be slightly stronger (i.e., faster warming) in models relative to observations (Rosenblum and Eisenman 2017; Roach et al. 2020). The impact of Southern Ocean sea surface temperatures (SSTs) on Antarctic sea ice has recently been investigated by Zhang et al. (2020), who found that, over 1979-2013, Southern Ocean cooling reduced Antarctic SIE loss in a GCM simulation but could not alone explain observed trends.

In this work, we assess the impact that winds have on Antarctic sea ice using a novel approach in which winds are nudged toward observed winds in a fully coupled Earth system model (ESM) run under historical forcing and anthropogenic emissions. This framework aims to eliminate the role of biases in winds (mean state, trends, and internal variability) on sea ice trends and variability. We also run simulations in which both winds and Southern Ocean SSTs north of the sea ice edge are nudged to observations. The questions that we address in this work are the following: How much can winds explain Antarctic sea ice mean state, trends, and variability? What is the impact of Southern Ocean SST trends on Antarctic sea ice? What is the influence of initial conditions on long-term sea ice trends?

2. Methods and data

For observations, we use three different products of satellite-derived sea ice concentration (SIC) in the Southern Ocean to sample uncertainty in retrieval algorithms (Ivanova et al. 2014; Eisenman et al. 2014): the NSIDC bootstrap (Comiso et al. 1997), NASA team (Cavalieri et al. 1997), and EUMETSAT Ocean and Sea Ice Satellite Application Facility (OSI SAF; Lavergne et al. 2019) sea ice products. We use the ERA-Interim dataset (Dee et al. 2011) to sample observed winds and surface temperature, and the NOAA Extended Reconstruction Sea Surface Temperature version 3b (ERSSTv3b) product for SSTs (Smith et al. 2008).

We use the National Center for Atmospheric Research (NCAR) Community Earth System Model version 1 with the Community Atmosphere Model version 5 (CESM1-CAM5; Hurrell et al. 2013). The model features fully coupled atmosphere, ocean, sea ice, and land components at a ~1° resolution, and is among the CMIP5 models with highest fidelity compared to observations (Knutti et al. 2013). We use the Large Ensemble performed with CESM1-CAM5 (hereafter referred to as CESM-LENS; Kay et al. 2015) which consists of 35 members initialized in 1920 with atmospheric initial conditions that differ at round-off level.

For the nudging simulations, we select initial conditions from CESM-LENS from 1 January 1980. Thereafter, we run the model under historical forcing from 1979 to 2005 and RCP8.5 from 2006 to 2018 (identical to the CESM-LENS forcing). We nudge model zonal (U) and meridional (V) winds to 6-hourly ERA-Interim U and V winds poleward of 45° in both hemispheres (i.e., over 45°–90°N and 45°–90°S) throughout the full period (January 1979 to December 2018). In a subset of simulations, we also nudge model SSTs to observations over the Southern Ocean north of the sea ice edge between 40° and 56°S. The nudging [also termed relaxation approach in the literature; see e.g., Jung et al. (2014) and references therein] is performed by adding an extra term to the model as follows:

$$\frac{dx}{dt} = F(x) + F_{\text{nudge}},$$

$$F_{\text{nudge}} = \alpha [O(t'_{\text{next}}) - x(t)]/\tau,$$
(1)

where x(t) is the model state vector at model time step t; F(x) is the internal tendency of the system with no nudging; and $F_{\rm nudge}$ is the nudging term, proportional to the difference between the target analysis (e.g., ERA-Interim winds) at a future analysis time step, $O(t'_{\rm next})$, and the model state at the current model time step, x(t). In the atmosphere, the analysis that the model is nudged toward is updated every 6 h (the analysis time step $t'_{\rm next}$) while $F_{\rm nudge}$ is adjusted at each model time step (in CAM5, $\Delta t = 30$ min). The nudging coefficient α is 1 everywhere within the nudging domain and changes to 0 smoothly across the nudging domain border as shown in Fig. 1, and τ is the relaxation time scale $\tau = t'_{\rm next} - t$ of the nudging, that is, the time between the current model time step (t) and the following analysis (observations) time step ($t'_{\rm next}$) that the model is nudged toward.

To nudge the model to observed Southern Ocean SSTs, we follow the methodology of Kosaka and Xie (2013) whereby the model's SSTs are nudged to the observed monthly SST anomalies (with respect to the model mean) over the Southern Ocean (40°–56°S; i.e., north of the sea ice). A fixed relaxation time scale of 2 days is used and the nudging is applied to the model's top-10-m-deep ocean layer. The simulations that nudge SSTs also apply the wind nudging described above; we use $\alpha_{(U,V)}$ and $\alpha_{(SST)}$ to distinguish between the wind and SST nudging parameters. All experiments are described in Table 1, and each represents a single simulation.

We test the sensitivity of the nudging simulations to the magnitude of nudging parameter $\alpha_{(U,V)}$ and the range of vertical levels over which U and V are nudged. We nudge the winds at two different ranges of atmospheric levels. One range is from 850 hPa to the top of the model (TOM), denoted as CESM-NudgeUV, and the other range is all atmospheric levels, denoted CESM-NudgeUV_surf. In all nudging simulations that nudge winds above 850 hPa, downward momentum transfer and mass conservation constrain surface winds in the nudging simulations to closely match ERA-Interim surface winds, and over the Southern Ocean the correlation of monthly mean U and V winds between ERA-Interim and the nudged simulations is r > 0.97 (not

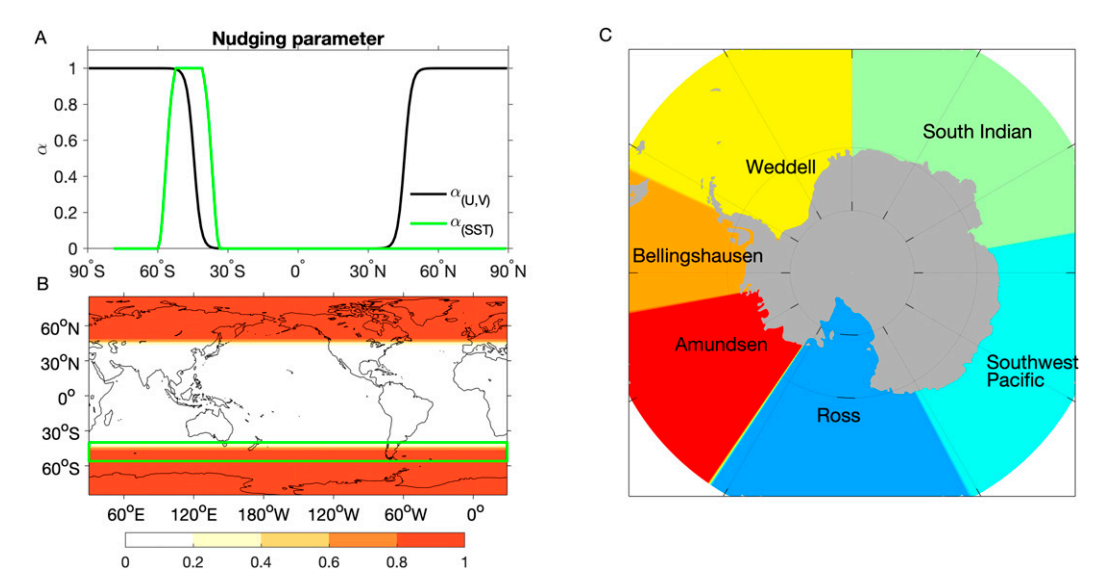


FIG. 1. (a) Nudging parameters for the winds $[\alpha_{(U,V)}]$ and SSTs $[\alpha_{(SST)}]$, (b) nudging domains for $\alpha_{(U,V)}$ (shaded) and $\alpha_{(SST)}$ (green box), and (c) the regional boundaries and nomenclature used.

shown). CESM-NudgeUV_surf experienced a slight climate drift, which can result from the nudging (e.g., Greatbatch et al. 2012; Blanchard-Wrigglesworth and Ding 2019), and we exclude this simulation from further analysis. Using a weaker nudging parameter $\alpha_{(U,V)}$ (CESM-NudgeUV_weak) results in an almost identical simulation to CESM-NudgeUV, and we also exclude this simulation from further analysis. To test the influence of initial conditions on long-term sea ice trends, we run a simulation that is initialized with sea ice concentrations from the CESM-LENS member with lowest 1980 sea ice conditions (denoted CESM-NudgeUV_lowIC) as opposed to CESM-NudgeUV, which is initialized from a CESM-LENS member with average 1980 sea ice conditions. Finally, to assess the impact of Southern Ocean SSTs, we run two additional simulations with the same parameters as CESM-NudgeUV and CESM-NudgeUV_lowIC that in addition apply SST nudging over a Southern Ocean domain, and we denote these as CESM-NudgeUV&SST and CESM-NudgeUV& SST_lowIC. To refer to both wind-only nudging simulations together, we use CESM-NudgeX, and to refer to both wind and SST nudging simulations together we use CESM-NudgeSSTX.

We assess sea ice both on pan-Antarctic and regional scales with different seas defined in Fig. 1c. For the regional analysis, all SIC data (observations and model output) are regridded to a common 1° latitude × 1° longitude grid prior to analysis. SIE is defined as the area of SIC greater than 15%, and sea ice area (SIA) as the area-integrated SIC. We assess statistical significance using a 95% confidence level calculated with Student's *t* test. We discuss results on 1) mean state, 2) trends, 3) coupling to temperature, and 4) interannual variability. We find that CESM-NudgeSSTX shares similar characteristics to CESM-NudgeX in terms of mean state and interannual variability, so we focus on CESM-NudgeX and discuss CESM-NudgeSSTX when investigating the relationship between sea ice and temperature.

3. Results

a. Mean state and evolution over 1979–2018

We first analyze the mean state of sea ice cover and winds in observations, CESM-LENS, and CESM-NudgeX. Note that we show the ensemble-mean of CESM-LENS, representing the forced response in the model. Figure 2 shows the mean

TABLE 1. Summary of model simulations. In all simulations, the nudging parameter $\alpha_{(U,V)}$ is applied over 45°-90°N and 45°-90°S.

Model ID	Initial conditions (with LENS run indicated)	$lpha_{(U,V)}$	Vertical nudging levels	SST nudging
CESM-NudgeUV	1980 climatological sea ice (LENS#21)	1	TOM to 850 hPa	_
CESM-NudgeUV_lowIC	1980 minimum sea ice (LENS#4)	1	TOM to 850 hPa	_
CESM-NudgeUV&SST	1980 climatological sea ice (LENS#21)	1	TOM to 850 hPa	40°-56°S
CESM-NudgeUV&SST_lowIC	1980 minimum sea ice (LENS#4)	1	TOM to 850 hPa	40°-56°S
CESM-NudgeUV_surf	1980 climatological sea ice (LENS#21)	1	TOM to surface	_
CESM-NudgeUV_weak	1980 climatological sea ice (LENS#21)	0.5	TOM to 850 hPa	_

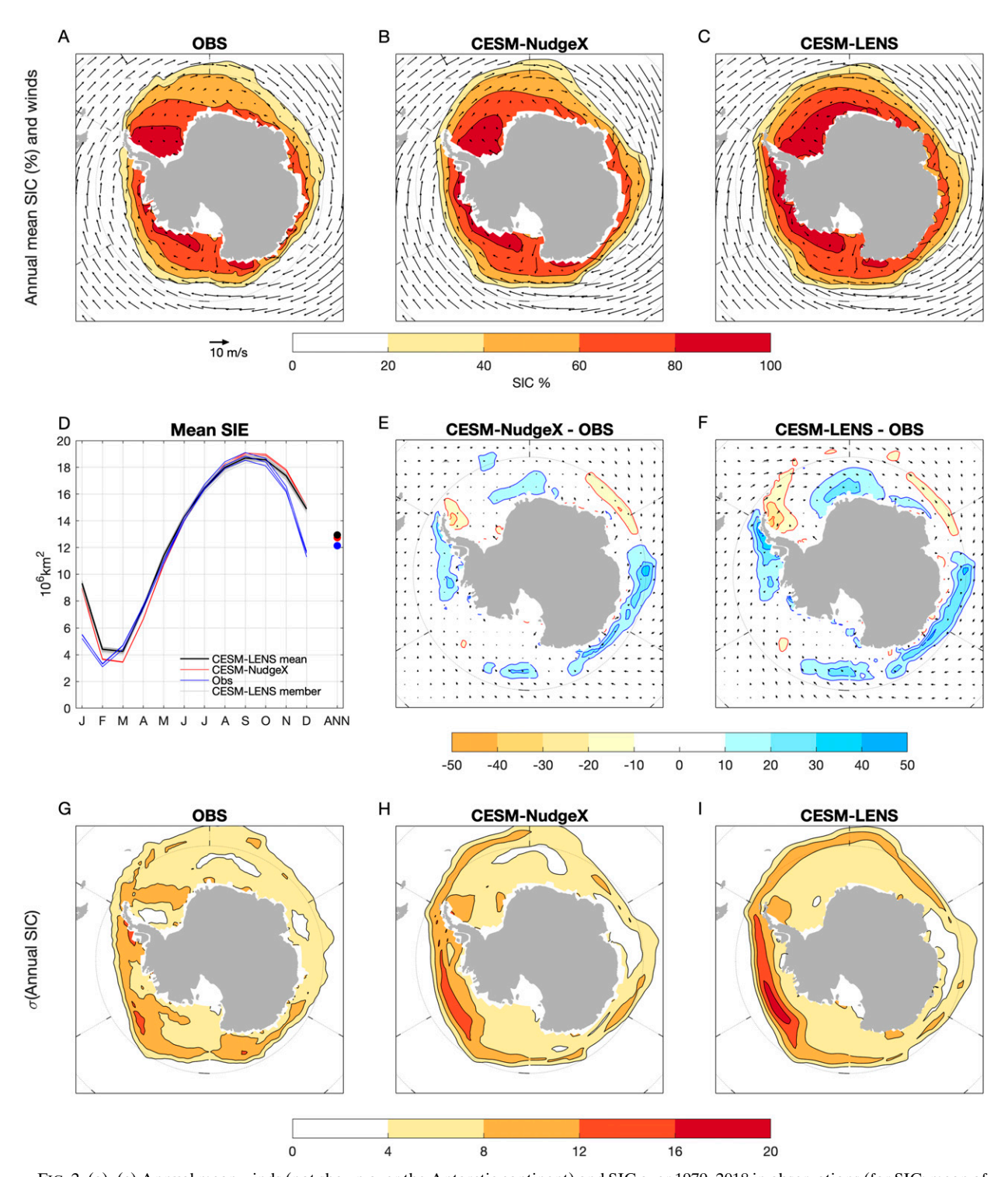


FIG. 2. (a)—(c) Annual mean winds (not shown over the Antarctic continent) and SIC over 1979–2018 in observations (for SIC: mean of Bootstrap, NASA team, and OSI SAF estimates), CESM-NudgeX, and CESM-LENS, (d) the seasonal cycle of SIE (all three observed SIE estimates shown), (e),(f) the differences in annual mean winds and SIC between model simulations and observations, and (g)—(i) the standard deviation of annual mean SIC.

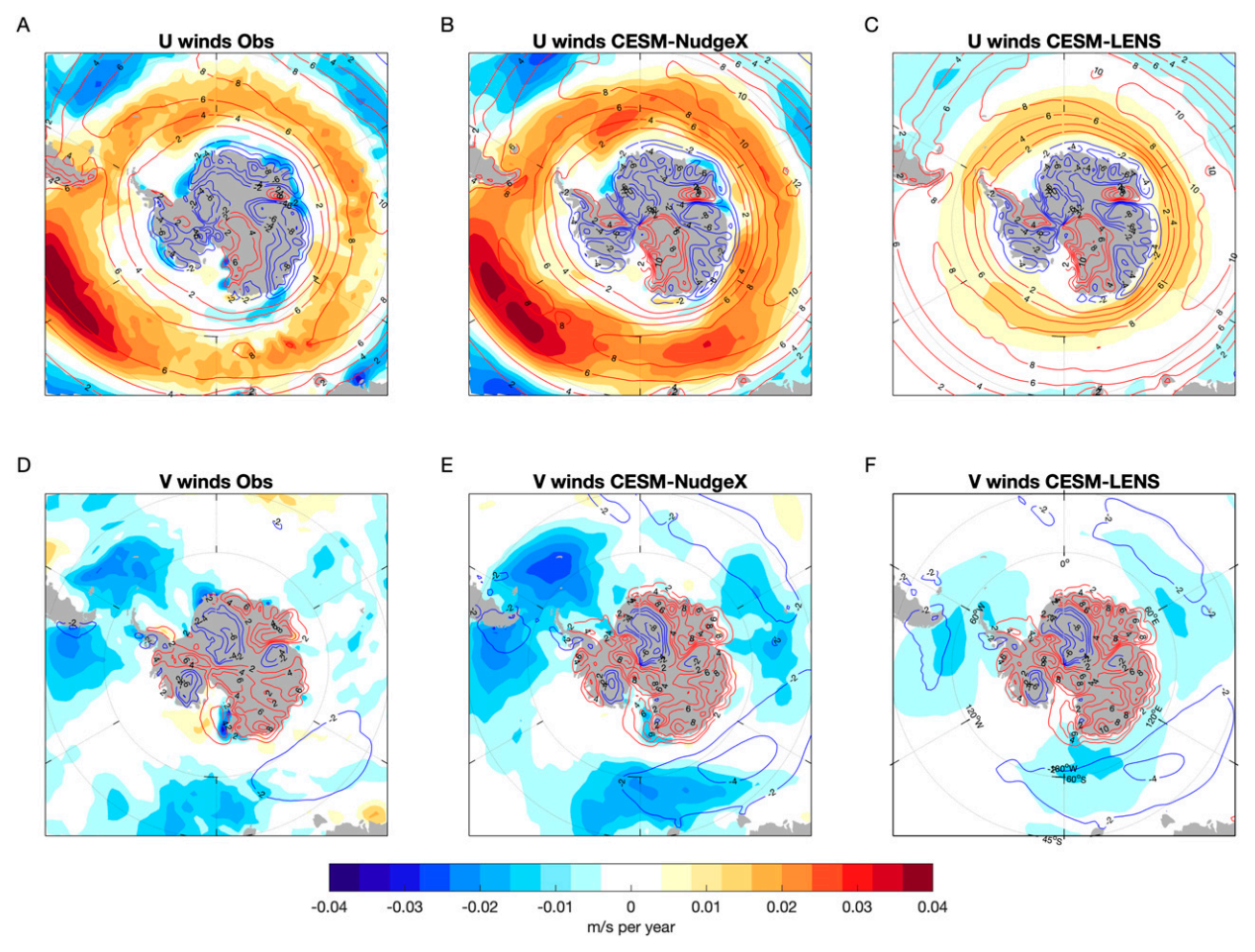


FIG. 3. Trends (in m s⁻¹ yr⁻¹; shading) and means (in m s⁻¹; contours) over 1979–2018 of annual surface (a)–(c) zonal U winds (positive is westerly) and (d)–(f) meridional V winds (positive is southerly) in (left) observations, (middle) CESM-NudgeX, and (right) CESM-LENS.

annual SIC and surface winds in observations, CESM-LENS and CESM-NudgeX, ensemble-mean model biases, the seasonal cycle of SIE, and the standard deviation of annual mean SIC in all three different datasets. We show seasonal mean and biases in SIC and winds in Fig. S1 in the online supplemental material. Throughout the year, both CESM-LENS and CESM-NudgeX skillfully simulate the seasonal cycle of Antarctic SIE, with a notable exception during spring, when observations show a faster loss in SIE (Fig. 2d). CESM-LENS and CESM-NudgeX show a positive bias in mean annual SIE, with annual SIE about 0.8×10^6 and 0.6×10^6 km² greater than observations, respectively. In terms of the spatial distribution of SIC, the model simulations show a positive bias in SIC in the southwest Pacific Ocean and the Ross, Amundsen, and Bellingshausen Seas, and a negative bias in SIC in the western Weddell Sea and south Indian Ocean. CESM-LENS shows slightly stronger zonal winds over the Southern Ocean, and these biases are mostly corrected in CESM-NudgeX, especially north of West Antarctica, the Antarctic Peninsula, and the Weddell Sea. Comparing the biases in SIC in CESM-NudgeX with those in CESM-LENS shows an improvement in the Weddell and Bellingshausen Seas and the southwest Pacific, where model biases are approximately halved, but no discernible changes elsewhere. Model biases in the rate of SIE loss during the spring originate in SIC biases along the marginal sea ice zone of the southwest Pacific and the Ross Sea (see Fig. S1 in the online supplemental material) and remain unchanged in CESM-NudgeX relative to CESM-LENS, despite improvement of winds in CESM-NudgeX over these regions in spring, suggesting that the spring SIE bias does not result from model wind biases.

The standard deviation in annual SIC for the three datasets is calculated first for each single observation and model simulation, and then averaged across observations and individual model simulations/ensemble members (Figs. 2g-i). The observations show a maximum in variability along the Bellingshausen, Amundsen, and Ross Seas, and reduced variability (about a third to a half lower) from the eastern Weddell Sea to the east Pacific (0° to 120°E). CESM-LENS shows a similar pattern, but in general overestimates interannual SIC variability. CESM-NudgeX shows an improvement in variability relative to CESM-LENS, but still slightly overestimates observed variability.

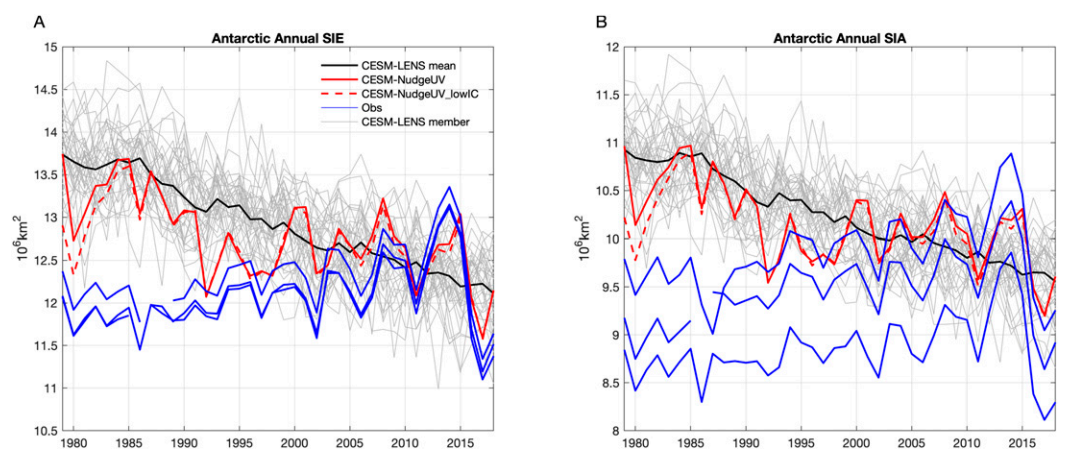


FIG. 4. Annual mean (a) SIE and (b) SIA over 1979–2018 in observations (blue), CESM-NudgeUV (red), CESM-NudgeUV_lowIC (dashed red), and CESM-LENS (ensemble mean in black, individual runs in gray) in Antarctica.

From this mean state analysis, and in the context of large model uncertainty in simulating Antarctic sea ice (Turner et al. 2013; Roach et al. 2020), we argue that CESM-LENS performs reasonably well in capturing the mean state of Antarctic sea ice, and that CESM-NudgeX shows that winds modestly improve the mean state of sea ice.

Figure 3 shows annual trends and means over 1979–2018 in surface U and V winds in observations (as estimated in ERA-Interim), CESM-NudgeX, and CESM-LENS. In observations, mean zonal winds show strong westerlies over the Southern Ocean north of the sea ice edge that peak in the south Indian sector, while along the Antarctic coastline zonal winds are weak or easterly. CESM-LENS shows a similar pattern, although with slightly stronger westerlies over the Southern Ocean, particularly during the spring (Fig. S1). Trends over the last 40 years in observations show a strengthening of the westerly winds over the Southern Ocean, a poleward migration of the strongest winds in the South Indian sector, an equatorward migration over the southeast Pacific, and a weak strengthening of the easterlies along the Antarctic coastline. The strongest trends are located in the southeast Pacific. Mean meridional winds are much weaker than zonal winds over the Southern Ocean, and their trends show a weak wave-3 pattern with strengthening northerlies centered around 60°W, 60°E, and 180°E. Trends in zonal winds in CESM-LENS (averaged across all members) also show a strengthening of the westerlies, but much weaker than observations and located farther south, indicating a poleward migration of the westerlies at all longitudes. Unlike observations, the coastal easterlies show no trends, while CESM-LENS trends in meridional winds show a similar albeit weaker wave-3 pattern to observations. As expected given our experiment design, zonal and meridional wind trends in CESM-NudgeX follow closely the observed trends.

Annual mean Antarctic SIE and SIA in 1979–2018 for CESM-LENS, CESM-NudgeX, and observations are shown in Fig. 4 and for regional seas in Fig. 5. Observed Antarctic SIE and SIA show the previously documented increase over 1979–2015, and the rapid decrease and reduced sea ice cover over 2016–18. There is greater observational uncertainty in SIA relative to SIE.

The CESM-LENS mean shows a linear decrease in Antarctic SIE and SIA during this period, in agreement with other climate model response to global warming and anthropogenic forcing (e.g., Turner et al. 2013). Both CESM-NudgeUV and CESM-NudgeUV_lowIC show a pattern in SIE and SIA that is partitioned in three phases: a loss of sea ice over 1979–92, an increase in sea ice over 1992–2015, and a marked decrease, though smaller than observed, in 2016 and low sea ice conditions since. CESM-NudgeUV_lowIC shows slightly lower SIE and SIA relative to CESM-NudgeUV for the first 3 years, after which both simulations show very similar SIE and SIA.

At the regional scale (Fig. 5 for annual SIE; see Figs. S2 and S3 for seasonal and monthly SIE), observed SIE evolution patterns are distinct to the pan-Antarctic pattern shown in Fig. 4, and some seas show a long-term decrease (such as the Bellingshausen Sea). The CESM-NudgeX simulations capture the observed interannual variability and trends of SIE in the Bellingshausen, Amundsen, Weddell, and Ross Seas. In the southwest Pacific and south Indian Ocean, there is a larger discrepancy between CESM-NudgeX and observations. In both areas, CESM-NudgeX captures interannual variability, yet it shows a negative sea ice trend while observations show a positive sea ice trend, and CESM-NudgeX is seemingly constrained to the CESM-LENS ensemble range, which might help explain why CESM-NudgeX cannot simulate the increase in SIE in the south Indian Ocean in the 2000s. The origin for the smaller-than-observed decline in Antarctic SIE in 2016 in CESM-NudgeX is also the south Indian Ocean (see Figs. S2 and S3). CESM-LENS shows negative trends in all seas. We discuss regional trends and interannual variability further below.

b. Sea ice trends

1) Antarctic trends

We quantify the monthly and annual trends in Antarctic SIE in CESM-LENS, CESM-NudgeX, and observations in Fig. 6. In observations, over 1979–2018 SIE has increased during all

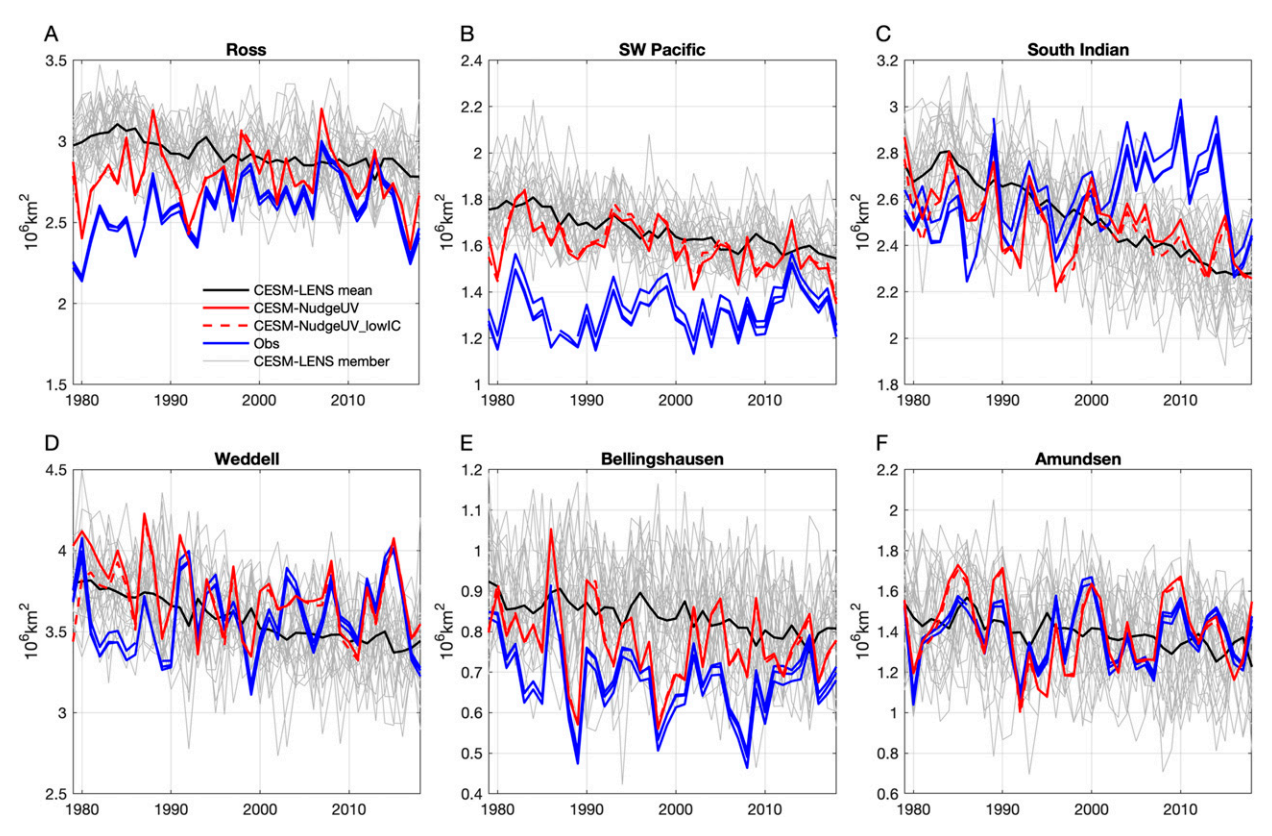


FIG. 5. Annual mean SIE in 1979–2018 in observations (blue), CESM-NudgeUV (red), CESM-NudgeUV_lowIC (dashed red), and CESM-LENS (ensemble mean in black, individual runs in gray) in regional seas of Antarctica.

seasons with weak seasonality in the trends, although the largest positive trends are during the fall and early winter (April through June) and trends are only statistically significant at the 95% level from May through October. The mean trend in annual SIE across observations is 0.011 \times $10^6\,\mathrm{km^2\,yr^{-1}}$, and only one of the three observational datasets shows a statistically significant annual SIE trend. In CESM-

LENS, all monthly and annual SIE trends are negative for all ensemble members, and they tend to be more pronounced during the late fall/winter relative to summer. Annual SIE trends are statistically significant in all ensemble members, and the observed trend is outside the range of model trends in all months. Both CESM-NudgeX simulations also have negative trends but the magnitude of trends is approximately one-half of

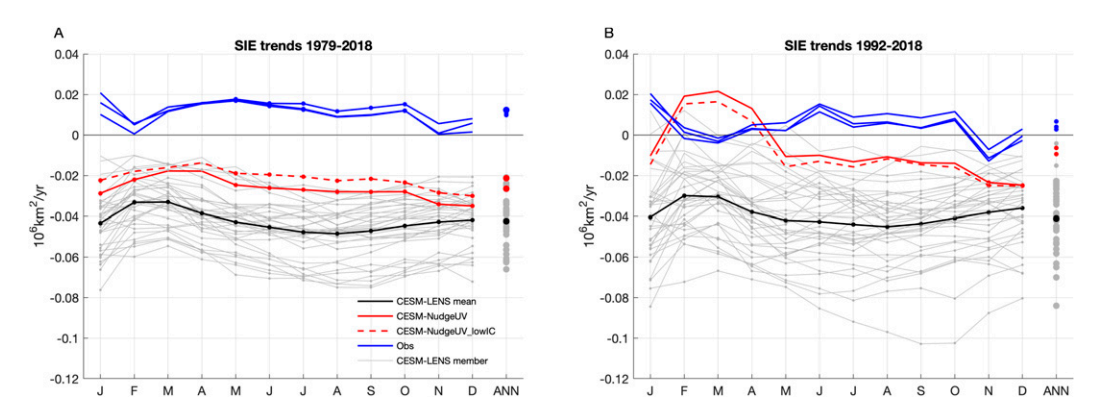


FIG. 6. Monthly and annual trends in SIE over (a) 1979–2018 and (b) 1992–2018 for observations (blue), CESM-NudgeUV (red), CESM-NudgeUV_lowIC (dashed red), and CESM-LENS (individual runs in gray, ensemble mean in black). Circular markers on monthly trends and larger markers for the annual trends indicate statistically significant trends at the 95% level.

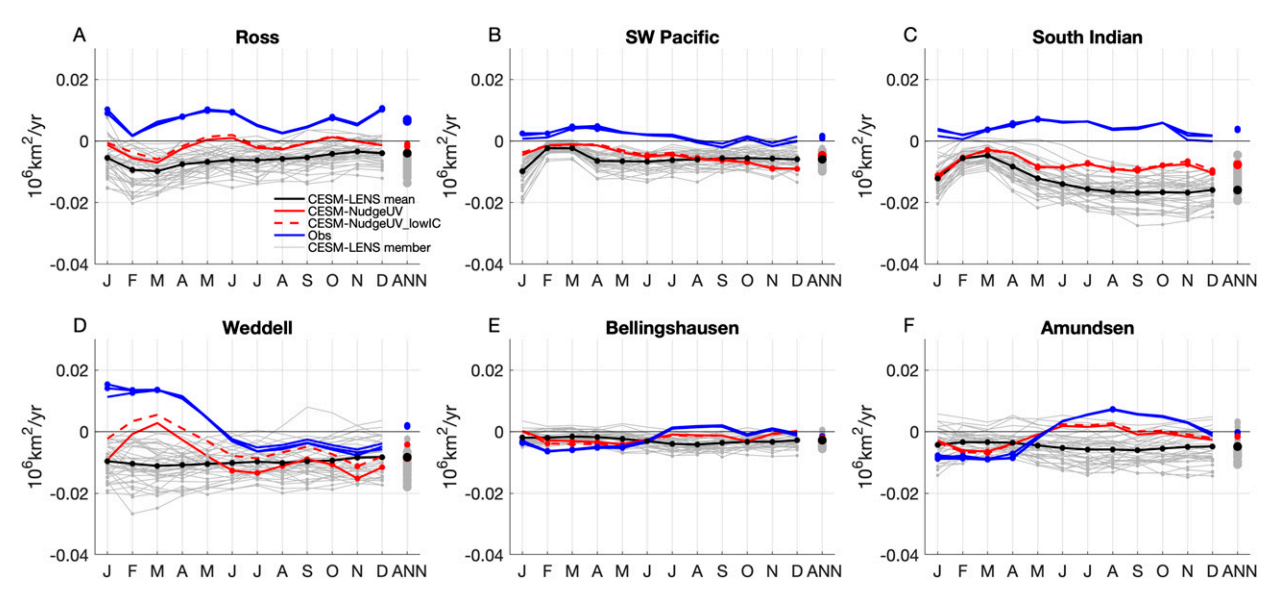
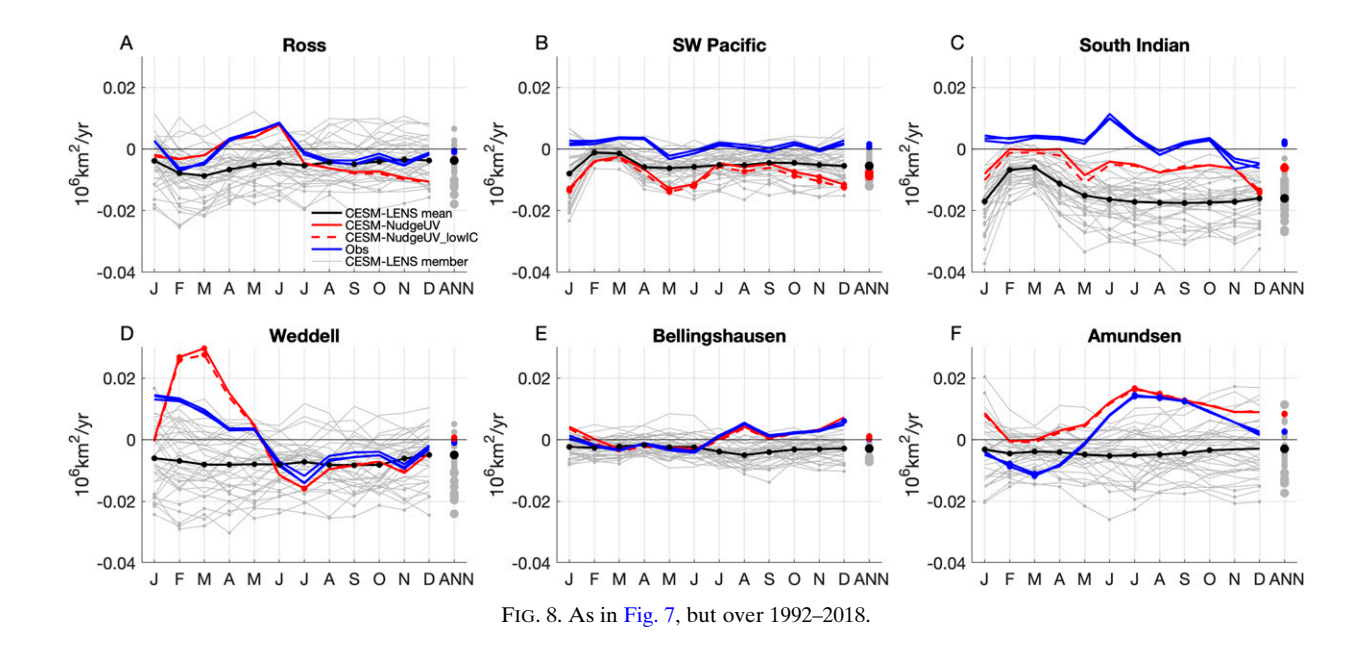


FIG. 7. Monthly and annual regional trends in SIE over 1979–2018 for observations (blue), CESM-NudgeUV (red), CESM-NudgeUV_lowIC (dashed red), and CESM-LENS (individual runs in gray, ensemble mean in black). Circular markers on monthly trends and larger markers for the annual trends indicate statistically significant trends at the 95% level.

that in CESM-LENS (annual SIE trend of -0.026×10^6 and $-0.021 \times 10^6 \, \mathrm{km^2 \, yr^{-1}}$ in CESM-NudgeUV and CESM-NudgeUV_lowIC respectively compared to $-0.043 \times 10^6 \, \mathrm{km^2 \, yr^{-1}}$ for CESM-LENS). As in observations, late summer/early fall SIE trends in CESM-NudgeX are not statistically significant, and trends in both nudged simulations are at the high end of the individual CESM-LENS ensemble member trends.

Given the apparent shift in trends in the early 1990s in CESM-NudgeX shown in Fig. 4, we also quantify SIE trends over 1992–2018 (Fig. 6b). During this period, observed trends

in annual SIE are smaller than over 1979–2018 (0.005 \times $10^6\,\mathrm{km^2\,yr^{-1}}$ compared to $0.011\times10^6\,\mathrm{km^2\,yr^{-1}}$) and are not statistically significant. Both CESM-NudgeUV and CESM-NudgeUV_lowIC have slightly negative annual trends ($-0.0033\times10^6\,\mathrm{km^2\,yr^{-1}}$ and $-0.0059\times10^6\,\mathrm{km^2\,yr^{-1}}$, respectively), which are also not statistically different from zero. The CESM-LENS mean trend during this time is an order of magnitude greater ($-0.039\times10^6\,\mathrm{km^2\,yr^{-1}}$). The trends in both CESM-NudgeX simulations are positive during the late summer/early fall (February through April), about a season earlier than the most positive trends in observations, although



we note that no monthly SIE trends in observations and CESM-NudgeX (with the exception of November and December in the latter) are statistically different from zero.

2) REGIONAL TRENDS

Observed regional trends in sea ice cover show a complex pattern both in terms of spatial and seasonal trends, with some Antarctic seas such as the Ross Sea showing a marked long-term increase in sea ice cover while others such as the Bellingshausen Sea show a decrease in sea ice (e.g., Holland 2014; Comiso et al. 2017; Parkinson 2019). These regional differences in sea ice trends have been linked to regional differences in wind trends, as some regions have shown an increase in northerly winds and others have shown an increase in southerly winds, yet the relationship between winds and sea ice cover is complex, as wind trends in one season (e.g., spring) can affect sea ice trends in another season (e.g., fall) (e.g., Holland 2014; Holland et al. 2017b), and sea ice anomalies can be advected from one region to another (e.g., Pope et al. 2017).

Figure 7 shows monthly and annual trends in regional SIE over 1979-2018, highlighting where and when the observational trends are outside the range of CESM-LENS and in what regions nudging to observed winds can at least partially reconcile the observation-model mismatch. In the Weddell Sea, observed positive summer/fall SIE trends are followed by negative winter SIE trends, while the Amundsen and Bellingshausen Seas show negative summer SIE trends (which are more negative than the range of trends simulated by CESM-LENS) and positive winter SIE trends. In the Bellingshausen and Amundsen Seas, CESM-NudgeX replicates observed trends skillfully. In the Weddell and Ross Seas and the southwest Pacific, CESM-NudgeX captures the observed seasonality of SIE trends, but in general is biased negative relative to observations. In the south Indian Ocean, CESM-NudgeX trends are more biased with respect to observed trends, showing a year-round loss in SIE compared to a year-round increase in observations.

Repeating this analysis over 1992–2018 (Fig. 8) shows that during this more recent period, CESM-NudgeX captures observed trends with a high degree of skill throughout the year in the Bellingshausen, Amundsen, Ross, and Weddell Seas. In the southwest Pacific and south Indian Ocean, CESM-NudgeX underestimates trends for all months, as was seen over 1979–2018 in Fig. 7.

To complement the spatial analysis of sea ice trends, Figs. 9 and 10 show seasonal and annual trends in SIC over 1979–2018 and 1992–2018 in the ensemble-mean of CESM-LENS (which represents the model's forced response), CESM-NudgeX, and observations together with the trends in surface winds over the same time periods. We also show seasonal and annual trends in SIA by longitude (defined as the trend in SIA calculated for each degree of longitude) in all three datasets and across all CESM-LENS members.

Overall, CESM-NudgeX captures observed trends in the Bellingshausen and Amundsen Seas over 1979–2018, and the Ross and Weddell Seas over 1992–2018. In contrast, observed positive SIE trends in the southwest Pacific and south Indian Ocean are not captured by CESM-NudgeX. At the annual time scale zonal winds have increased (become more westerly) in observations, a pattern that is much weaker in the CESM-LENS ensemble-mean. Trends in seasonally averaged winds,

however, show a deepening of the Amundsen low in summer and particularly in fall in observations that is absent in the CESM-LENS ensemble-mean, likely illustrating a model bias as this deepening has partly been attributed to changes in ozone and simulated in other climate models (Turner et al. 2009) (we note that CESM-LENS forcing includes changes in ozone). This deepening of the Amundsen low has resulted in increased southerlies over the Ross and Amundsen Seas, and increased northerlies over the Bellingshausen Sea during these seasons. Inspecting the trends in winds and their relationship to SIC trends, however, shows a complex pattern. For example, in fall, Weddell Sea SIC trends over 1979-2018 are mostly positive, despite stronger northerly winds, while Amundsen SIC trends are negative, despite a trend of stronger southerly winds, and in the following season, Amundsen SIC trends are positive, despite no clear trends in meridional winds. This likely highlights the delayed response of sea ice to wind (e.g., Holland et al. 2017b) and the seasonal persistence of sea ice that likely extends sea ice trends from one month to the next despite changes in the overlying atmospheric forcing: thus, it is likely that the negative fall SIC trends in the Amundsen Sea partly result from the negative summer SIC trends in that region. Comparing the longitudinal SIA trends over 1992-2018 in Fig. 10 to Fig. 9 shows the improvement in regional skills in CESM-NudgeX during this period. The skill during winter over 1992-2018, when CESM-NudgeX captures the wave-3 pattern of observed SIC trends, is particularly noteworthy. During this season and over this period, CESM-NudgeX simulates positive trends in longitudinal SIA that are outside the range of CESM-LENS trends in the Amundsen Sea and in the western sector of the south Indian Ocean.

c. Coupling of sea ice and temperature

Over decadal and longer time scales, Antarctic sea ice is coupled to global and hemispheric temperature in ESMs (e.g., Armour et al. 2011; Rosenblum and Eisenman 2017; Roach et al. 2020). In Fig. 11 we show annual mean surface (2 m) air temperature and SST from ERA-Interim/ErSSTv3b, CESM-LENS, and CESM-NudgeX, and the relationship between annual SIE trends and trends in mean annual temperature averaged over the globe and Southern Hemisphere and trends in SST averaged over a Southern Ocean domain north of the sea ice edge (48°-56°S). Annual mean temperature over all three domains has warmed at a greater rate in CESM-LENS compared to observations. As expected given the nudging experiment design, CESM-NudgeX temperatures are within the range of CESM-LENS temperature, and thus show a similar long-term warming. The difference in SST trends over the Southern Ocean domain between ErSSTv3b and CESM-LENS is particularly noteworthy, as the observed cooling is outside the range of modeled trends (Fig. 11c; Fig. S4 shows annual SST trend maps). Scatterplots of temperature trends and sea ice trends show that Antarctic sea ice trends in CESM-LENS are coupled to temperature/SST trends, not only over the Southern Ocean but in the Southern Hemisphere and globally. Importantly, the relationships between temperature trends and Antarctic SIE trends that account for differences across the individual LENS members also help account for the differences between SIE trends in observations and models (including the nudged simulations), especially so when considering Southern Hemisphere and Southern Ocean

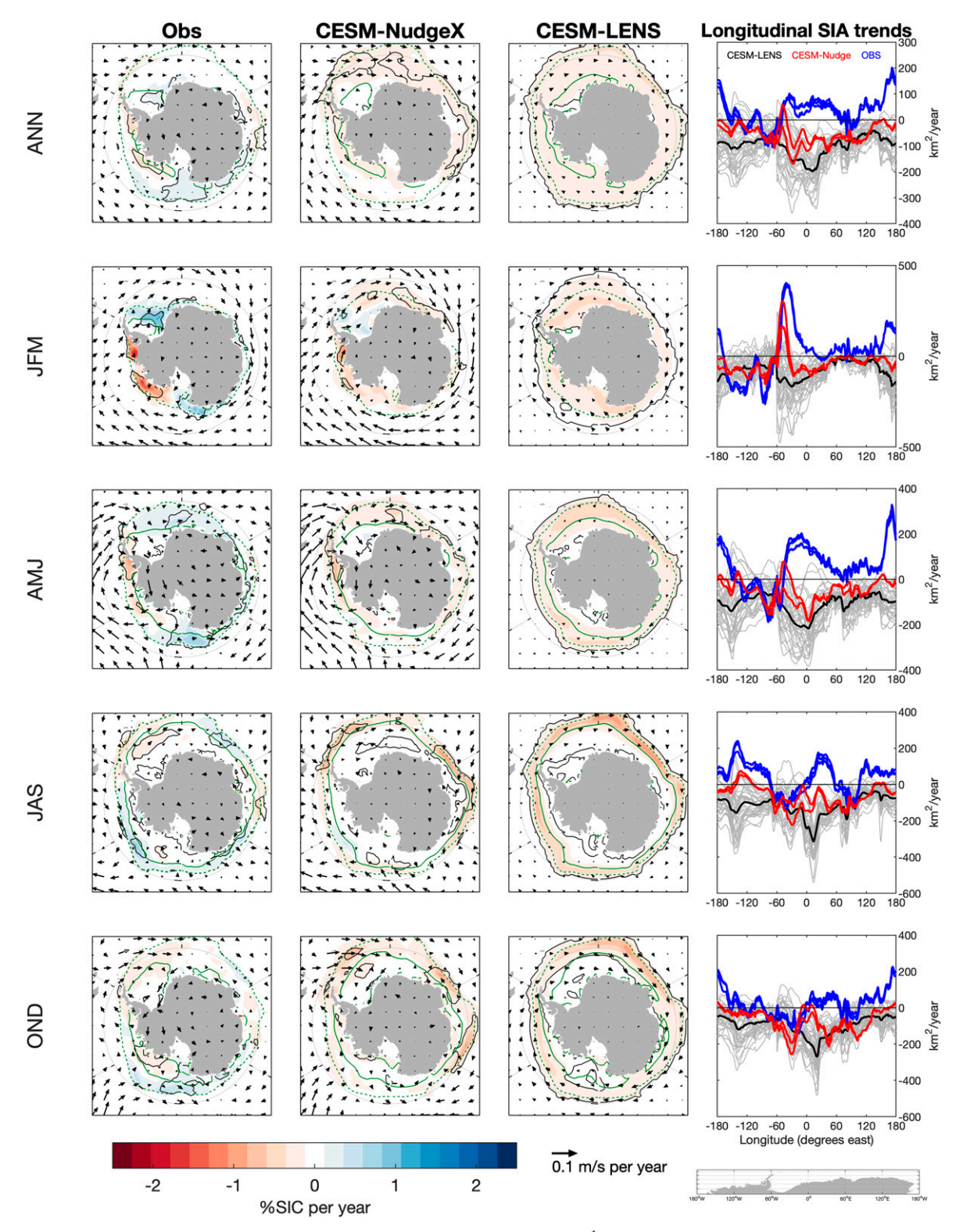


FIG. 9. (left three columns) Annual and seasonal SIC concentration trends (% yr⁻¹) and trends in winds in Antarctica over 1979–2018 in observations, CESM-NudgeX, and CESM-LENS mean, respectively. The dashed and continuous green lines denote the mean 15% and 80% SIC contours, respectively, and the black contours indicate statistically significant trends at the 95% level. (right) Longitudinal SIA trends in observations (blue), CESM-NudgeX (red), and CESM-LENS (gray, ensemble mean in black). (bottom right) The Antarctic coastline is aligned with the longitudinal SIA trend panels above it to aid geographic interpretation.

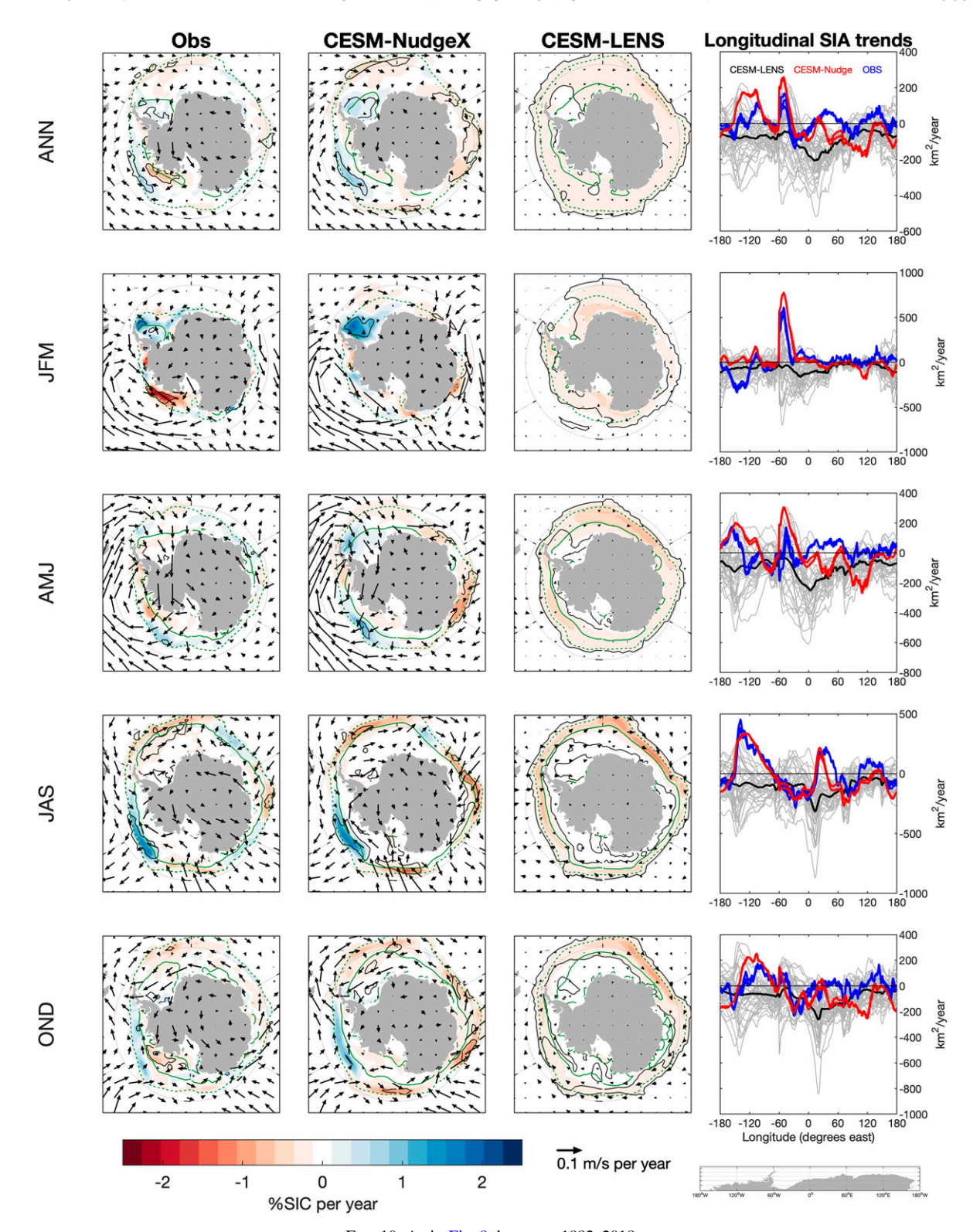


FIG. 10. As in Fig. 9, but over 1992–2018.

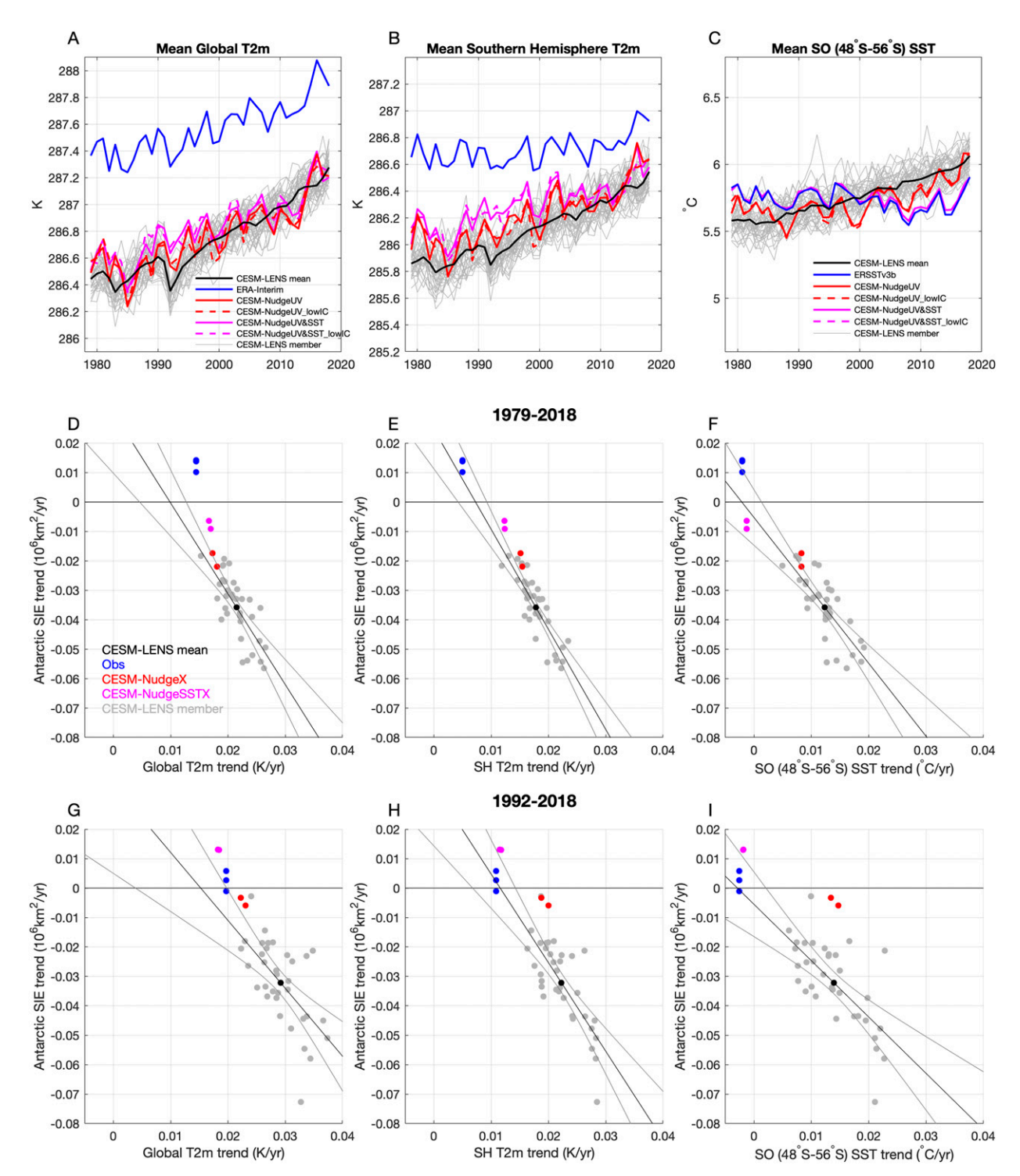


FIG. 11. (a)–(c) Annual mean global, Southern Hemisphere (SH), and Southern Ocean domain (48°–56°S) surface 2-m air temperature (T2m) and SST over 1979–2018 (note the *y*-axis range is the same for all three panels). Also shown are scatterplots of trends in global, SH and Southern Ocean temperatures and Antarctic SIE over (d)–(f) 1979–2018 and (g)–(i) 1992–2018. Best-fit linear regression and its 95% confidence intervals of the CESM-LENS members data are shown by the black and gray lines in (d)–(i).

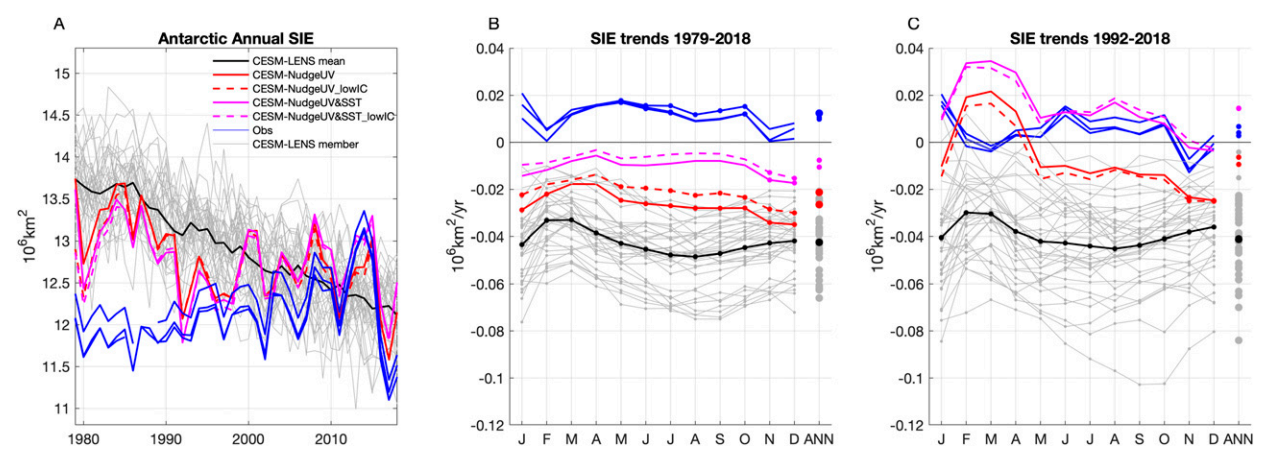


FIG. 12. As in Figs. 4a and 6, but including CESM-NudgeSSTX.

temperature trends (Figs. 11e,f). This suggests that the inability of CESM-NudgeX to reproduce observed Antarctic SIE trends over the longer 1979-2018 period results from the coupling of the Southern Ocean to the larger scale climate system and the toorapidly warming global and hemispheric-scale temperatures in CESM-LENS and CESM-NudgeX. Over the shorter 1992-2018 period, the difference in temperature trends between ERA-Interim and CESM-LENS/CESM-NudgeX is smaller relative to the 1979-2018 period. Additionally, the coupling between sea ice and largescale temperature trends is weaker than that over the longer period (the correlations are weaker in the lower panels of Fig. 11) and the SIE trends in CESM-NudgeX do not conform to the relationship seen across the CESM-LENS simulations. This result suggest that wind trends exert a larger influence on SIE trends on shorter time scales while climate-scale thermodynamic controls are more important at longer time scales.

IMPACT OF SOUTHERN OCEAN SSTS

As shown in Fig. 11f and Fig. S4, Southern Ocean SSTs north of the sea ice warm at a faster rate in CESM-LENS than observations, and wind-nudging slightly improves this warming bias in CESM-NudgeX. To investigate the impact of these model biases on sea ice trends we turn to CESM-NudgeSSTX. Figure 12 shows time series of Antarctic SIE and trends in CESM-NudgeSSTX, observations, CESM-LENS, and CESM-NudgeX (see Figs. S2 and S3 for monthly and seasonal SIE). The interannual variability of SIE in CESM-NudgeSSTX follows that in CESM-NudgeX closely, and SIE longterm trends are slightly more positive in CESM-NudgeSSTX, with 1979–2018 annual SIE trends of -0.011×10^6 and $-0.008 \times$ 10⁶ km² yr^{−1} in CESM-NudgeSST and CESM-NudgeSST_lowIC, respectively, compared to -0.026×10^6 and -0.021×10^6 km² yr⁻¹ in CESM-NudgeUV and CESM-NudgeUV_lowIC, respectively. Neither CESM-NudgeSSTX annual SIE trend is significantly different from zero over the 1979-2018 and 1992-2018 periods. Inspection of regional SIE and SIE trends (Figs. S5-S7) shows an improvement in simulated SIE trends in CESM-NudgeSSTX compared to CESM-NudgeX in the south Indian Ocean and Weddell Sea, while elsewhere trends are mostly unchanged between CESM-NudgeSSTX and CESM-NudgeX. The relationship between temperature and sea ice trends in CESM-NudgeSSTX in Fig. 11

provides further evidence of the coupling between temperature and sea ice and the impact of Southern Ocean SSTs on Antarctic SIE trends, particularly over the longer 1979–2018 period.

d. Sea ice interannual variability

We next explore how well CESM-NudgeX captures interannual sea ice variability. We show the correlations of monthly and annual Antarctic and regional SIE between the CESM-NudgeX and observations in Fig. 13 over 1979-2018 and 1992-2018. For simplicity, and given the agreement in variability within the observational SIE estimates, and CESM-NudgeX (see Fig. 4), we show the mean values of all six single correlation matrices (i.e., the combination of three observational estimates and two nudged simulations). The correlation between CESM-NudgeX and observations in pan-Antarctic annual SIE over 1979–2018 is $r \sim 0.2$, and $r \sim 0.5$ when both CESM-NudgeX and observed SIE are detrended. There is a seasonal cycle as CESM-NudgeX captures interannual variability of pan-Antarctic SIE better during the freeze-up (April-June) and melt (December-January) seasons. During the 1992-2018 period, the correlation pattern is similar with slightly higher correlation values, especially for pan-Antarctic SIE (cf. left columns in Figs. 13c,d and 13a,b), when $r \sim 0.66$ ($r \sim 0.68$ for detrended) for annual SIE. We note that CESM-NudgeSSTX shows similar results (see Fig. S8) and improved correlations prior to SIE detrending, as expected from the improved simulation of SIE trends shown in Fig. 12 (the correlation between CESM-NudgeSSTX and observations in pan-Antarctic annual SIE is $r \sim 0.4$).

As suggested by a visual comparison of Figs. 4 and 5, CESM-NudgeX tends to capture observed interannual variability better at the regional scale (in Figs. S2 and S3, we show seasonal and monthly SIE in CESM-NudgeX, CESM-NudgeSSTX, and observations). The correlation between CESM-NudgeX and observations in regional annual SIE varies between r > 0.8 for the Bellingshausen and Amundsen Seas and $r \sim 0.3$ for the south Indian Ocean over 1979–2018. When the annual time series are detrended, correlations are higher in those regions where CESM-NudgeX and observations show diverging trends (i.e., the southwest Pacific and south Indian Ocean; cf. Fig. 5).

At the monthly time scale, two patterns emerge in terms of seasonality and geography in Fig. 13. Seasonally, CESM-NudgeX

В

<SIE Obs

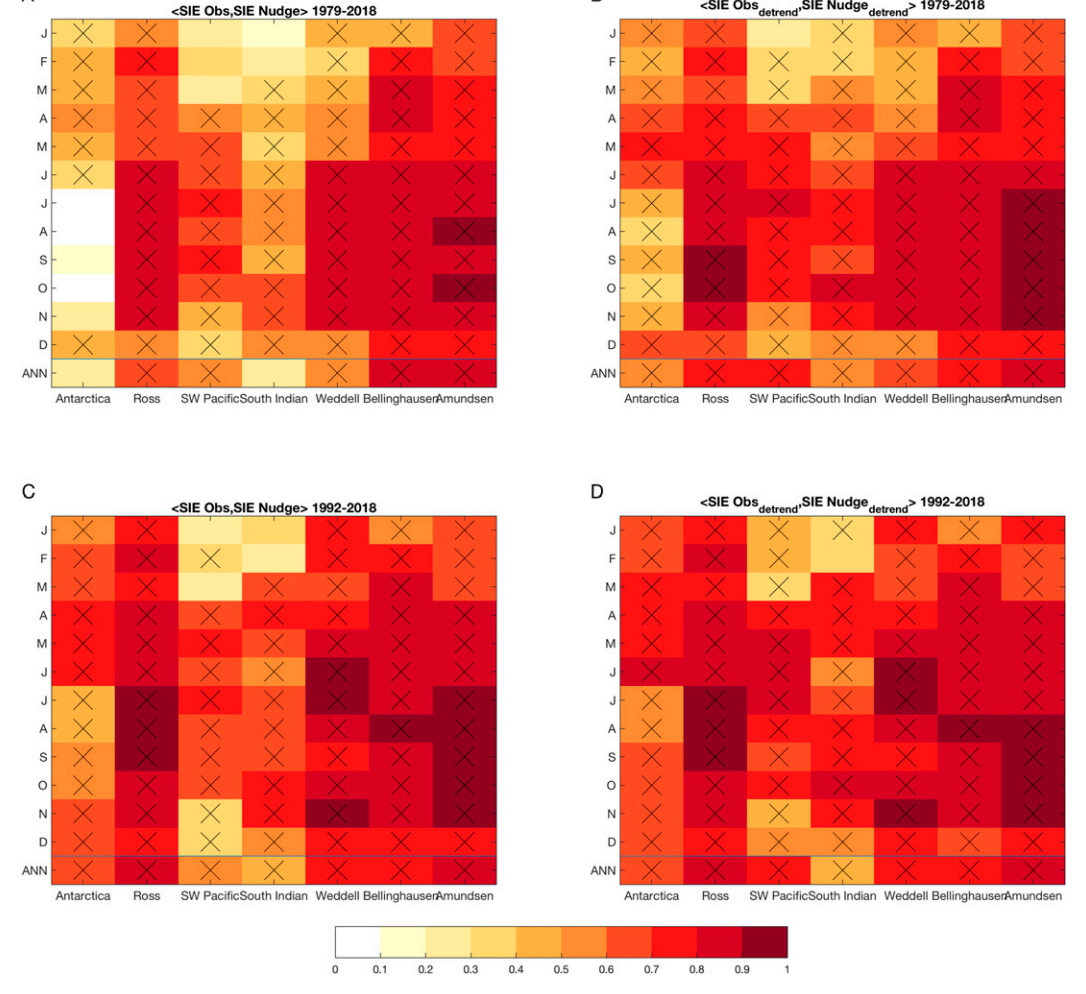


FIG. 13. Correlation r values of monthly and annual Antarctic and regional SIE between CESM-NudgeX and observations over (a),(b) 1979-2018 and (c),(d) 1992-2018 (a),(c) without detrending the time series and (b),(d) after linearly detrending. Hatched values indicate statistically significant correlations at a 95% level.

captures observed regional SIE variability better during winter and spring (April through November) compared to summer and early fall (December through March). During the winter months, correlation values between CESM-NudgeX and observations can be greater than r = 0.9 in the Ross, Amundsen, Bellingshausen, and Weddell Seas. Interestingly, this seasonality in regional SIE skill is different from the seasonality for pan-Antarctic SIE skill. Geographically, CESM-NudgeX captures variability better over the Weddell, Ross, Amundsen, and Bellingshausen Seas relative to the southwest Pacific and south Indian Ocean. This is the same geographic pattern of CESM-NudgeX skill in capturing observed regional trends documented above.

4. Discussion and conclusions

A

We have used a fully coupled climate model with its winds nudged to observations over 1979-2018 to investigate the impact of winds on Antarctic sea ice mean state, trends, and variability. We have also explored the additional impact on sea ice trends of Southern Ocean SSTs north of the sea ice by nudging the model's SSTs to observations. Model sea ice mean state biases are only modestly improved by nudging winds to observations (CESM-NudgeX compared to CESM-LENS). Specifically, the slower than observed melt during the spring in CESM-LENS persists in CESM-NudgeX, suggesting that this model bias does not originate from biased winds but rather from biased thermodynamics. At the pan-Antarctic scale, we show improvement in CESM-NudgeX compared to CESM-LENS in capturing the observed SIE trends, and further improvement when the model is nudged to both winds and Southern Ocean SSTs in CESM-NudgeSSTX. The latter show no significant trends in SIE over 1979-2018, in agreement with two of the three observed estimates of SIE trends.

Observed SIE trends are better captured in CESM-NudgeX after the early 1990s, as the nudged simulations simulate an increase in SIE up to 2015 and a marked decline since. In contrast, the model shows a loss in SIE over the 1980s that is not seen in observations. CESM-NudgeX also captures observed interannual variability in Antarctic SIE with moderate success ($r \sim 0.5$ for annual SIE over 1979–2018 after linearly detrending, $r \sim 0.68$ over 1992–2018). The simulated SIE decline in austral spring 2016 is slightly smaller than observed, due principally to a larger observed decline in the south Indian Ocean, which may not be attributable to winds (see also Fig. 2A in Meehl et al. 2019).

At the regional scale, CESM-NudgeX shows significant skill in capturing the observed trends, especially after the early 1990s, and very good skill in capturing interannual variability in SIE throughout the full 1979–2018 period. In some regions and months, the correlation between simulated and observed SIE is r > 0.9. Regional trends in CESM-NudgeSSTX are similar to CESM-NudgeX, but show an improvement in the Weddell Sea and south Indian Ocean. A geographic and seasonal pattern in skill is clear, whereby CESM-NudgeX skill is better in the Ross/Amundsen/Bellingshausen Seas, and to some extent the Weddell Sea relative to the southwest Pacific and south Indian Ocean, while skill in the winter and spring months is better relative to late summer and early fall. What might be the source of this geographic and seasonal diversity? Could sea ice in the former regions, and in winter, be more strongly constrained by winds relative to other processes (such as ocean currents or local atmospheric radiative forcing)? Could the fidelity of reanalysis winds themselves be lower in the latter regions? Regarding the first hypothesis, we note that the differences between the CESM-NudgeUV and CESM-NudgeUV_lowIC simulations are very small across all regions and seasons (see Fig. 5 and Figs. S2 and S3). We might expect that if sea ice in some regions showed less influence from winds, the intermodel spread in the nudging simulations would be greater. The near-identical evolution of sea ice in both nudging simulations implies that, at least in the model, sea ice is highly constrained by winds (directly or by other processes that covary with winds) in all regions and seasons. Nevertheless, Holland and Kwok (2012) found that in observations sea ice motion is less strongly coupled to winds along East Antarctica, but we note that this pattern could also result from larger uncertainty in the wind reanalysis in East Antarctica (see below). Comparing nudging simulations with different initial conditions shows no impact on long-term SIE trends. This result is somewhat surprising in light of Zhang et al. (2019), who found using a GFDL-based ESM that decadal sea ice trends depend on the initial conditions and are conditioned by the state of Southern Ocean deep convection during initialization. We note that CESM1-CAM5 does not simulate deep convection in the Southern Ocean (de Lavergne et al. 2014), and thus our result may be conditioned by this model feature of CESM1-CAM5.

Given the scarcity of surface stations and radiosondes around Antarctica and the Southern Ocean, quantifying regional variations in the skill of reanalysis products is not trivial. Jones et al. (2016), in a validation of reanalysis with radiosondes not assimilated into the reanalysis in the Amundsen Sea region, found that reanalyses struggle to capture orographic and katabatic enhancements of the winds. These processes are more relevant along the East Antarctic coastline than over open ocean far from land and West Antarctica, and may help

explain the lower skill in SIE in the CESM-NudgeX simulations in late summer/early fall and in the south Indian Ocean and southwest Pacific when the sea ice edge is closer to the East Antarctic coastline. Regarding the fidelity of reanalysis winds themselves, we note that there exists large uncertainty across different reanalysis products in simulated sea level pressure fields across the southern ocean (e.g., Jones and Lister 2007; Hobbs et al. 2016). Additionally, satellite scatterometers, which are the main source of surface wind information over the open ocean, have only been operational and their data assimilated into reanalysis since 1992 (Dee et al. 2011; Desbiolles et al. 2017), which may help account for the change in model skill in capturing wind-driven sea ice trends before and after that date. However, the nudged simulations capture regional interannual SIE variability with high skill throughout the whole period (Figs. 5 and 13), which might suggest no major degradation in the fidelity of ERA-Interim winds prior to 1992. Nevertheless, since the signal of interannual variability is greater than that for trends, it is not necessarily contradictory that the fidelity of reanalysis winds prior to the scatterometer era may be high enough to capture interannual variability but too low to accurately capture low-frequency trends. To assess the impact of reanalysis fidelity on our nudged simulations, additional simulations that nudge to winds taken from different reanalysis products are needed.

Notwithstanding issues of reanalysis wind fidelity, it is important to note that surface air temperature and SST trends in CESM-LENS and CESM-NudgeX are significantly more positive than in observations (as indicated by ERA-Interim and ERSSTv3b). Particularly over the Southern Ocean north of the sea ice edge, observed SST 1979-2018 trends are negative, while all CESM-LENS and CESM-NudgeX trends are positive. Given the coupling between sea ice trends and temperature trends at decadal time scales, it is perhaps not surprising that CESM-NudgeX does not simulate a 40-yr-long positive trend in SIE against a backdrop of rapidly warming temperatures, echoing the findings of Schneider and Deser (2018). These findings are further supported by CESM-NudgeSSTX; in these simulations, reduced Southern Ocean warming leads to more positive SIE trends relative to CESM-NudgeX. Over 1992-2018, however, ERA-Interim and CESM temperature trends are in closer agreement over the SO, and during this shorter time period sea ice trends are less strongly coupled with temperature trends, two factors that perhaps help explain the improved skill of CESM-NudgeX in capturing more recent trends in sea ice. We note that the relationship between sea ice and temperature is not necessarily indicative of a causal effect between temperature trends and sea ice trends, as recent work has shown that Antarctic sea ice loss can also modulate global temperature (e.g., England et al. 2020).

Overall, our results illustrate the key role that winds have played in the recent trends and interannual variability of sea ice across Antarctica, and thus are a key component in understanding changes in the region. However, winds alone cannot explain the absence of sea ice loss over 1979–2018, and only when combined with observed SST trends over the Southern Ocean north of the sea ice does the model simulate a near-zero trend in SIE over 1979–2018. The skill of projections

of future decadal trends and shorter time-scale forecasts of Antarctic sea ice thus likely depends on capturing future changes in winds and in Southern Ocean SSTs. Furthermore, the nudging methodology employed showcases a new pathway for exploring sea ice-atmosphere interactions, model bias diagnosis, and reanalysis fidelity assessment, and we plan future work to investigate the sensitivity of our results to the choice of climate model and reanalysis product.

Acknowledgments. We would like to acknowledge high-performance computing support from Cheyenne (doi:10.5065/D6RX99HX) provided by NCAR's Computational and Information Systems Laboratory, sponsored by the National Science Foundation. We also acknowledge support from Patrick Callaghan of NCAR, who developed the atmospheric nudging module for CAM, and Sally Zhang and Nan Rosenbloom of NCAR, who provided support with the SST nudging methodology. We thank Mitch Bushuk for discussion and Andrew Pauling for technical support. E.B.W. and A.D., were supported by the National Science Foundation (NSF) Antarctic Program PLR1643436, L.R., was supported by NSF Grant PLR-1643431LR, and Q.D., was supported by NSF's Polar Programs OPP-1744598.

Data availability statement. The CESM-LENS data are publicly available (see http://www.cesm.ucar.edu/projects/community-projects/LENS/data-sets.html) and ERA-Interim data were accessed via NCAR's Research Data Archive (https://rda.ucar.edu/). The CESM-NudgeX output is available via NCAR Cheyenne (contact authors for details).

REFERENCES

- Armour, K. C., I. Eisenman, E. Blanchard-Wrigglesworth, K. McCusker, and C. Bitz, 2011: The reversibility of sea ice loss in a state-of-the-art climate model. *Geophys. Res. Lett.*, 38, L16705, https://doi.org/10.1029/2011GL048739.
- —, J. Marshall, J. R. Scott, A. Donohoe, and E. R. Newsom, 2016: Southern Ocean warming delayed by circumpolar upwelling and equatorward transport. *Nat. Geosci.*, 9, 549–554, https://doi.org/10.1038/ngeo2731.
- Bintanja, R., G. van Oldenborgh, S. Drijfhout, B. Wouters, and C. Katsman, 2013: Important role for ocean warming and increased ice-shelf melt in Antarctic sea-ice expansion. *Nat. Geosci.*, **6**, 376–379, https://doi.org/10.1038/ngeo1767.
- Bitz, C., and L. M. Polvani, 2012: Antarctic climate response to stratospheric ozone depletion in a fine resolution ocean climate model. *Geophys. Res. Lett.*, 39, L20705, https://doi.org/ 10.1029/2012GL053393.
- Blanchard-Wrigglesworth, E., and Q. Ding, 2019: Tropical and midlatitude impact on seasonal polar predictability in the Community Earth System Model. J. Climate, 32, 5997–6014, https://doi.org/10.1175/JCLI-D-19-0088.1.
- Bronselaer, B., M. Winton, S. M. Griffies, W. J. Hurlin, K. B. Rodgers, O. V. Sergienko, R. J. Stouffer, and J. L. Russell, 2018: Change in future climate due to Antarctic meltwater. Nature, 564, 53–58, https://doi.org/10.1038/s41586-018-0712-z.
- Cavalieri, D., C. Parkinson, P. Gloersen, and H. Zwally, 1997: Arctic and Antarctic sea ice concentrations from multichannel passive-microwave satellite data sets: October 1978 to September 1995. NASA Tech. Memo. 104627, 17 pp., https://nsidc.org/sites/

- nsidc.org/files/technical-references/NASA%20Technical%20Memorandum%20104647.pdf.
- Comiso, J. C., D. J. Cavalieri, C. L. Parkinson, and P. Gloersen, 1997: Passive microwave algorithms for sea ice concentration: A comparison of two techniques. *Remote Sens. Environ.*, 60, 357–384, https://doi.org/10.1016/S0034-4257(96)00220-9.
- ——, R. A. Gersten, L. V. Stock, J. Turner, G. J. Perez, and K. Cho, 2017: Positive trend in the Antarctic sea ice cover and associated changes in surface temperature. *J. Climate*, 30, 2251–2267, https://doi.org/10.1175/JCLI-D-16-0408.1.
- Dee, D. P., and Coauthors, 2011: The ERA-Interim reanalysis: Configuration and performance of the data assimilation system. *Quart. J. Roy. Meteor. Soc.*, **137**, 553–597, https://doi.org/10.1002/qj.828.
- de Lavergne, C., J. B. Palter, E. D. Galbraith, R. Bernardello, and I. Marinov, 2014: Cessation of deep convection in the open Southern Ocean under anthropogenic climate change. *Nat. Climate Change*, 4, 278–282, https://doi.org/10.1038/nclimate2132.
- Desbiolles, F., and Coauthors, 2017: Two decades [1992–2012] of surface wind analyses based on satellite scatterometer observations. *J. Mar. Syst.*, **168**, 38–56, https://doi.org/10.1016/j.jmarsys.2017.01.003.
- Eisenman, I., W. N. Meier, and J. R. Norris, 2014: A spurious jump in the satellite record: Has Antarctic sea ice expansion been overestimated? *Cryosphere*, 8, 1289–1296, https://doi.org/ 10.5194/tc-8-1289-2014.
- England, M. R., L. M. Polvani, L. Sun, and C. Deser, 2020: Tropical climate responses to projected Arctic and Antarctic sea-ice loss. *Nat. Geosci.*, 13, 275–281, https://doi.org/10.1038/s41561-020-0546-9.
- Ferreira, D., J. Marshall, C. M. Bitz, S. Solomon, and A. Plumb, 2015: Antarctic ocean and sea ice response to ozone depletion: A two-time-scale problem. *J. Climate*, 28, 1206–1226, https://doi.org/10.1175/JCLI-D-14-00313.1.
- Greatbatch, R. J., G. Gollan, T. Jung, and T. Kunz, 2012: Factors influencing Northern Hemisphere winter mean atmospheric circulation anomalies during the period 1960/61 to 2001/02. *Quart. J. Roy. Meteor. Soc.*, 138, 1970–1982, https://doi.org/10.1002/qj.1947.
- Hobbs, W. R., R. Massom, S. Stammerjohn, P. Reid, G. Williams, and W. Meier, 2016: A review of recent changes in Southern Ocean sea ice, their drivers and forcings. *Global Planet. Change*, 143, 228–250, https://doi.org/10.1016/j.gloplacha.2016.06.008.
- Holland, M. M., L. Landrum, Y. Kostov, and J. Marshall, 2017a: Sensitivity of Antarctic sea ice to the Southern Annular Mode in coupled climate models. *Climate Dyn.*, 49, 1813–1831, https://doi.org/10.1007/s00382-016-3424-9.
- —, —, M. Raphael, and S. Stammerjohn, 2017b: Springtime winds drive Ross Sea ice variability and change in the following autumn. *Nat. Commun.*, 8, 731, https://doi.org/10.1038/s41467-017-00820-0.
- Holland, P. R., 2014: The seasonality of Antarctic sea ice trends. Geophys. Res. Lett., 41, 4230–4237, https://doi.org/10.1002/ 2014GL060172.
- —, and R. Kwok, 2012: Wind-driven trends in Antarctic sea-ice drift. Nat. Geosci., 5, 872–875, https://doi.org/10.1038/ngeo1627.
- Hurrell, J. W., and Coauthors, 2013: The Community Earth System Model: A framework for collaborative research. *Bull. Amer. Meteor. Soc.*, 94, 1339–1360, https://doi.org/10.1175/BAMS-D-12-00121.1.
- Ivanova, N., O. M. Johannessen, L. T. Pedersen, and R. T. Tonboe, 2014: Retrieval of Arctic sea ice parameters by satellite passive microwave sensors: A comparison of eleven sea ice concentration

- algorithms. *IEEE Trans. Geosci. Remote Sens.*, **52**, 7233–7246, https://doi.org/10.1109/TGRS.2014.2310136.
- Jones, P. D., and D. H. Lister, 2007: Intercomparison of four different Southern Hemisphere sea level pressure datasets. *Geophys. Res. Lett.*, 34, L10704, https://doi.org/10.1029/ 2007GL029251.
- Jones, R. W., I. Renfrew, A. Orr, B. Webber, D. Holland, and M. Lazzara, 2016: Evaluation of four global reanalysis products using in situ observations in the Amundsen Sea Embayment, Antarctica. J. Geophys. Res. Atmos., 121, 6240– 6257, https://doi.org/10.1002/2015JD024680.
- Jung, T., M. A. Kasper, T. Semmler, and S. Serrar, 2014: Arctic influence on subseasonal midlatitude prediction. *Geophys. Res. Lett.*, 41, 3676–3680, https://doi.org/10.1002/2014GL059961.
- Kay, J., and Coauthors, 2015: The Community Earth System Model (CESM) large ensemble project: A community resource for studying climate change in the presence of internal climate variability. *Bull. Amer. Meteor. Soc.*, 96, 1333–1349, https:// doi.org/10.1175/BAMS-D-13-00255.1.
- Knutti, R., D. Masson, and A. Gettelman, 2013: Climate model genealogy: Generation CMIP5 and how we got there. Geophys. Res. Lett., 40, 1194–1199, https://doi.org/10.1002/grl.50256.
- Kohout, A., M. Williams, S. Dean, and M. Meylan, 2014: Storm-induced sea-ice breakup and the implications for ice extent. Nature, 509, 604–607, https://doi.org/10.1038/nature13262.
- Kosaka, Y., and S.-P. Xie, 2013: Recent global-warming hiatus tied to equatorial Pacific surface cooling. *Nature*, **501**, 403–407, https://doi.org/10.1038/nature12534.
- Lavergne, T., and Coauthors, 2019: Version 2 of the EUMETSAT OSI SAF and ESA CCI sea-ice concentration climate data records. *Cryosphere*, 13, 49–78, https://doi.org/10.5194/tc-13-49-2019.
- Liu, J., and J. A. Curry, 2010: Accelerated warming of the Southern Ocean and its impacts on the hydrological cycle and sea ice. *Proc. Natl. Acad. Sci. USA*, 107, 14 987–14 992, https://doi.org/ 10.1073/pnas.1003336107.
- Mahlstein, I., P. R. Gent, and S. Solomon, 2013: Historical Antarctic mean sea ice area, sea ice trends, and winds in CMIP5 simulations. J. Geophys. Res. Atmos., 118, 5105–5110, https://doi.org/10.1002/jgrd.50443.
- Meehl, G. A., J. M. Arblaster, C. M. Bitz, C. T. Chung, and H. Teng, 2016: Antarctic sea-ice expansion between 2000 and 2014 driven by tropical Pacific decadal climate variability. *Nat. Geosci.*, 9, 590–595, https://doi.org/10.1038/ngeo2751.
- —, —, C. T. Chung, M. M. Holland, A. DuVivier, L. Thompson, D. Yang, and C. M. Bitz, 2019: Sustained ocean changes contributed to sudden Antarctic sea ice retreat in late 2016. *Nat. Commun.*, **10**, 14, https://doi.org/10.1038/s41467-018-07865-9.
- Parkinson, C. L., 2019: A 40-y record reveals gradual Antarctic sea ice increases followed by decreases at rates far exceeding the rates seen in the Arctic. *Proc. Natl. Acad. Sci. USA*, 116, 14414–14423, https://doi.org/10.1073/pnas.1906556116.
- Polvani, L. M., and K. L. Smith, 2013: Can natural variability explain observed Antarctic sea ice trends? New modeling evidence from CMIP5. *Geophys. Res. Lett.*, 40, 3195–3199, https://doi.org/10.1002/grl.50578.
- Pope, J. O., P. R. Holland, A. Orr, G. J. Marshall, and T. Phillips, 2017: The impacts of El Niño on the observed sea ice budget of West Antarctica. *Geophys. Res. Lett.*, 44, 6200–6208, https:// doi.org/10.1002/2017GL073414.

- Purich, A., and M. H. England, 2019: Tropical teleconnections to Antarctic sea ice during austral spring 2016 in coupled pacemaker experiments. *Geophys. Res. Lett.*, 46, 6848–6858, https://doi.org/10.1029/2019GL082671.
- ——, and Coauthors, 2016: Tropical Pacific SST drivers of recent Antarctic sea ice trends. J. Climate, 29, 8931–8948, https://doi.org/10.1175/JCLI-D-16-0440.1.
- Roach, L. A., and Coauthors, 2020: Antarctic sea ice area in CMIP6. Geophys. Res. Lett., 47, e2019GL086729, https:// doi.org/10.1029/2019GL086729.
- Rosenblum, E., and I. Eisenman, 2017: Sea ice trends in climate models only accurate in runs with biased global warming. J. Climate, 30, 6265–6278, https://doi.org/10.1175/JCLI-D-16-0455.1.
- Schlosser, E., F. A. Haumann, and M. N. Raphael, 2018: Atmospheric influences on the anomalous 2016 Antarctic sea ice decay. *Cryosphere*, 12, 1103–1119, https://doi.org/10.5194/ tc-12-1103-2018.
- Schneider, D. P., and C. Deser, 2018: Tropically driven and externally forced patterns of Antarctic sea ice change: Reconciling observed and modeled trends. *Climate Dyn.*, **50**, 4599–4618, https://doi.org/10.1007/s00382-017-3893-5.
- Schroeter, S., W. Hobbs, and N. L. Bindoff, 2017: Interactions between Antarctic sea ice and large-scale atmospheric modes in CMIP5 models. *Cryosphere*, 11, 789–803, https://doi.org/ 10.5194/tc-11-789-2017.
- Sigmond, M., and J. Fyfe, 2010: Has the ozone hole contributed to increased Antarctic sea ice extent? *Geophys. Res. Lett.*, **37**, L18502, https://doi.org/10.1029/2010GL044301.
- Smith, T. M., R. W. Reynolds, T. C. Peterson, and J. Lawrimore, 2008: Improvements to NOAA's historical merged landocean surface temperature analysis (1880–2006). J. Climate, 21, 2283–2296, https://doi.org/10.1175/2007JCLI2100.1.
- Stuecker, M. F., C. M. Bitz, and K. C. Armour, 2017: Conditions leading to the unprecedented low Antarctic sea ice extent during the 2016 austral spring season. *Geophys. Res. Lett.*, 44, 9008–9019, https://doi.org/10.1002/2017GL074691.
- Thompson, D. W., and S. Solomon, 2002: Interpretation of recent Southern Hemisphere climate change. *Science*, **296**, 895–899, https://doi.org/10.1126/science.1069270.
- Turner, J., and Coauthors, 2009: Non-annular atmospheric circulation change induced by stratospheric ozone depletion and its role in the recent increase of Antarctic sea ice extent. *Geophys. Res. Lett.*, **36**, L08502, https://doi.org/10.1029/2009GL037524.
- ——, T. J. Bracegirdle, T. Phillips, G. J. Marshall, and J. S. Hosking, 2013: An initial assessment of Antarctic sea ice extent in the CMIP5 models. *J. Climate*, 26, 1473–1484, https://doi.org/10.1175/JCLI-D-12-00068.1.
- Zhang, J., 2007: Increasing Antarctic sea ice under warming atmospheric and oceanic conditions. J. Climate, 20, 2515–2529, https://doi.org/10.1175/JCLI4136.1.
- ——, 2014: Modeling the impact of wind intensification on Antarctic sea ice volume. J. Climate, 27, 202–214, https:// doi.org/10.1175/JCLI-D-12-00139.1.
- Zhang, L., T. L. Delworth, W. Cooke, and X. Yang, 2019: Natural variability of Southern Ocean convection as a driver of observed climate trends. *Nat. Climate Change*, 9, 59–65, https:// doi.org/10.1038/s41558-018-0350-3.
- Zhang, X., C, Deser, and L. Sun, 2020: Is there a tropical response to recent observed southern ocean cooling? Geophys. Res. Lett., 47, e2020GL091235, https://doi.org/10.1029/2020GL091235.